Passive coherent combining of CEP-stable few-cycles pulses from a temporally divided hollow fiber compressor

Hermance Jacqmin, Aurélie Jullien, Brigitte Mercier, Marc Hanna, Frédéric Druon, Dimitris N. Papadopoulos, Rodrigo B. Lopez-Martens

Passive coherent combining of CEP-stable few-cycle pulses from a temporally divided hollow fiber compressor

Hermance Jacqmin,[1,2,*] Aurélie Jullien,[1] Brigitte Mercier,[1] Marc Hanna,[3] Frédéric Druon,[3] Dimitrios Papadopoulos,[4] and Rodrigo Lopez-Martens[1]

[1]*Laboratoire d'Optique Appliquée, Ecole Nationale Supérieure de Techniques Avancées - Paristech, Ecole Polytechnique, CNRS, 91762 Palaiseau Cedex, France*

[2]*Thales Optronique SA, Laser Solutions Unit, 2 Avenue Gay-Lussac, 78995 Elancourt, France*

[3]*Laboratoire Charles Fabry, Institut d'Optique, CNRS, Université Paris-Sud, 91127 Palaiseau Cedex, France*

[4]*LULI, Ecole Polytechnique, CNRS, CEA, UPMC, 91128 Palaiseau, France*

**Corresponding author: hermance.jacqmin@ensta-paristech.fr*

Received November 28, 2014; revised January 12, 2015; accepted January 12, 2015; posted January 14, 2015 (Doc. ID 228509); published February 17, 2015

We demonstrate a simple and robust passive coherent combining technique for temporal compression of millijoule energy laser pulses down to few-cycle duration in a gas-filled hollow fiber. High combining efficiency is achieved by using carefully oriented calcite plates for temporal pulse division and recombination. Carrier-envelope phase (CEP)-stable, 6-fs, 800-nm pulses with more than 0.6 mJ energy are routinely generated. This method could aid in the energy scaling of CEP-stable hollow-fiber compressor systems.

OCIS codes: (320.7110) Ultrafast nonlinear optics; (320.5520) Pulse compression; (140.3298) Laser beam combining.
http://dx.doi.org/10.1364/OL.40.000709

Few-cycle pulses with stable carrier-envelope phase (CEP) constitute a unique tool for investigating and controlling electronic processes on the attosecond time scale [1]. One of the most popular techniques used for producing high spatial quality few-cycle pulses is nonlinear spectral broadening in a gas-filled hollow-core fiber followed by temporal compression with chirped mirrors [2,3]. However, as the input pulse energy approaches the milliJoule level, both the transmission and stability of hollow fiber compressors rapidly drop with the onset of self-focusing and ionization. The scaling of CEP-stable hollow fiber compressor systems to multimilliJoule energies typically requires the use of circularly polarized pulses and differentially pumped large cross-section fibers [4].

As shown by a recent theoretical study [5], an additional way of overcoming this limitation is to divide the input pulse into several lower energy replicas that can be subsequently recombined after independent spectral broadening in the fiber. Optical pulse multiplexing techniques have already been successfully demonstrated in the case of excimer amplifiers [6], fiber-chirped pulse amplification [7,8], optical parametric amplification [9], nonlinear compression in photonic crystal fibers [10,11], and sub-cycle waveform synthesizers [12]. To date, the shortest pulse duration obtained by coherent combining is 23 fs [13]. In this Letter, as a proof-of-principle experiment, we demonstrate the passive coherent combining of two temporally divided pulse replicas (500 μJ, 29 fs), spectrally broadened in a neon-filled hollow fiber compressor, with a combining efficiency of 95%. As a result, 6-fs post-compressed pulses with stable CEP are routinely generated using a simple and robust setup requiring no active beam stabilization. This is the first demonstration of optical multiplexing of few-cycle pulses in a hollow fiber compressor.

Working in the few-cycle regime imposes two main experimental constraints. First, low dispersion broadband optics must be used. Second, both temporal replicas must have identical optical beam paths through the fiber. Based on this, we use thin birefringent calcite plates for pulse division and combining. One configuration would involve making a roundtrip through the fiber using a single birefringent medium [10], but this means coupling the beam twice into the fiber and therefore increased losses. Moreover, the fraction of the beam that does not recombine can go back into the laser and deplete the amplifier medium or even damage it. A better solution is to make a single pass through the fiber and to use two separate calcite plates with carefully chosen crystallographic orientation. However, achieving high combination efficiency in this configuration requires that the delays introduced by the different calcite plates be strictly identical. One therefore needs to compensate for the potential difference in thickness between the two plates. Here, plate orientation plays an important role. Neglecting walk-off in the plates, the relative phase delay at 800 nm introduced between the two replicas can be expressed as

$$\tau = \frac{e}{c \times \cos\theta_{\mathrm{tilt}}}\left(n_o - \frac{1}{\sqrt{\frac{(\cos\theta)^2}{n_o^2} + \frac{(\sin\theta)^2}{n_e^2}}}\right), \qquad (1)$$

where e is the plate thickness and θ can be written as $\theta = \theta_c + \theta_{\mathrm{tilt}}$. θ_c is the crystallographic orientation of the plate (Fig. 1(a)), and θ_{tilt} is the experimental refracted angle inside the plate. There is a range of angles for which the relative phase delay varies linearly with θ. This offers a very sensitive degree of freedom for tuning both delays independently and correcting for the eventual difference in thickness between the two plates. This correction is possible when the ordinary axis of the first plate has the same orientation as the extraordinary axis of the second plate. Orienting these axes along the horizontal

0146-9592/15/050709-04$15.00/0

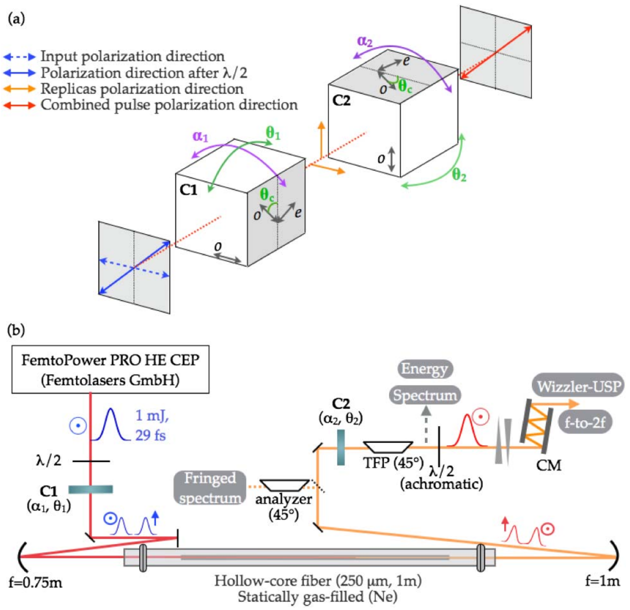

Fig. 1. (a) Polarization states through the calcite plates. (b) Experimental setup (C1, C2, calcite plates; TFP, thin film polarizer; CM, chirped mirrors).

direction enables adjusting the tilt of the second plate around the vertical rotation axis. Furthermore, the plates should be thin enough to minimize dispersion and nonlinear effects but thick enough so that replicas do not temporally overlap inside the fiber, thereby eliminating the possibility of cross-phase modulation. As underlined in [10], new wavelengths are created between pulse division and combination, requiring minimal GDD difference between both polarization components inside the plate used for combination. Taking all these considerations into account, we use 500 μm ± 50 μm-thick calcite plates with orientation $\theta_c = 45°$. Each surface is AR-coated (500–1000 nm). The calculated delay introduced is 150 fs assuming a constant crystallographic orientation of 45° and considering the index values found in the literature. This guarantees no overlap between the two 29 fs replicas. The average GDD is <50 fs^2, which can be easily compensated, and the GDD difference between the two polarization components is under 10 fs^2. For each plate (C1, C2), we define $\alpha_{1,2}$ as the rotation angle in the plate plane and $\theta_{1,2}$ as the tilt angle [Fig. 1(a)].

First, we determined the delay introduced by each calcite plate by measuring the fringed spectrum due to interferences between the two replicas and processing it with a Fourier transform. It was found that both C1 and C2 introduce an identical delay of 178 ± 0.5 fs.

The experimental setup is described in Fig. 1(b). A commercial FemtoPower (Femtolasers GmbH), including a CEP-stabilized oscillator with external frequency shifting in a feed-forward scheme, delivers 1-mJ, 29-fs pulses at 800 nm with a 1-kHz repetition rate. A half-wave plate (T>99%) turning the initial P-polarization at 45° is followed by the first calcite plate C1 (T≈97%) oriented at normal incidence ($\theta_1 = 0°$) with its ordinary axis oriented horizontally ($\alpha_1 = 90°$). The beam size is about 8 mm, and no spectral distortion occurs in the plate. The half-wave plate is adjusted so as to create two replicas with the same intensity, which is crucial since both pulses must undergo identical spectral broadening. This is achieved by minimizing spectral broadening when gas is added into the fiber. The accuracy on the orientation of the waveplate is 0.5°, which corresponds to an intensity difference between the replicas of less than 3.5%. The two orthogonally polarized replicas are focused into a 1-m-long statically neon-filled hollow fiber (T≈70%) with an inner diameter of 250 μm. After beam collimation at 8-mm diameter after the fiber, a first optional output is used to measure the fringed spectrum through an analyzer oriented at 45°. The beam then goes through the second calcite plate C2 (T≈97%) with its ordinary axis oriented vertically ($\alpha_2 = 0°$). A thin film polarizer (Femtolasers GmbH) (T>98%) discriminates the combined pulse and enables the measurement of both combining efficiency and combined pulse spectrum. With α_2, the optical axis of the second crystal can be adjusted parallel (perpendicular) to the polarization directions preventing further parasitic pulse division, which manifests itself by spectral modulations, while with θ_2, the exact timing can be obtained, as shown in Eq. (1). At this stage, the polarization direction of the combined pulse is 45°. A broadband half-wave plate is then used to recover P-polarization. Post-compression of the combined pulse is achieved using a pair of thin fused-silica wedges (70 fs^2) and a set of 12 double-angle chirped mirrors (–500 fs^2, UltraFast Innovations GmbH).

To investigate the effect of the degree of freedom θ_2, we recorded both combining efficiency and combined pulse spectrum for many values of this parameter without gas. The combining efficiency is calculated by dividing the energy measured after and before the TFP. The results are shown in Fig. 2(a). We observe

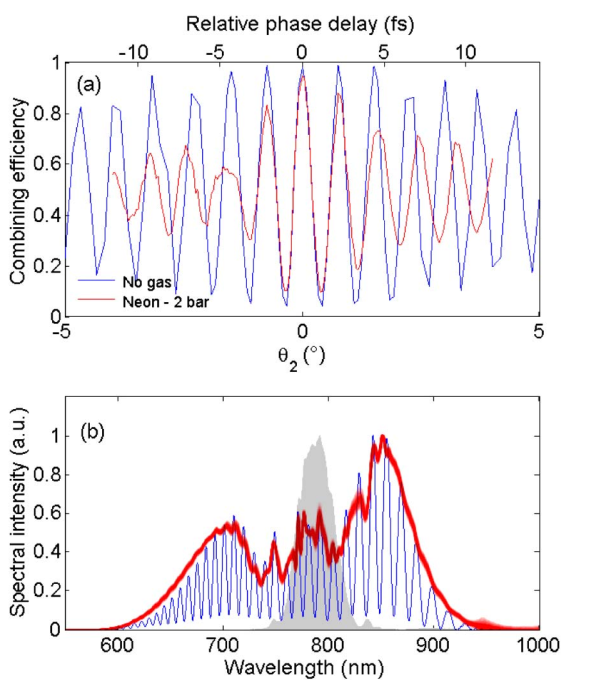

Fig. 2. (a) Evolution of the combining efficiency as a function of θ_2 with (red) and without gas (blue). (b) Initial laser spectrum (shaded area). Combined pulse spectra (500 scans, red) and fringed spectrum (blue) are registered for 2-bar Ne pressure.

regular constructive and destructive interferences, meaning that the combining process can be controlled with high precision. The best combining efficiency is 98%, which corresponds to the nominal transmission of the TFP. The θ_2 value obtained for the best combining efficiency is very close to the auto-collimation position as expected. The required resolution on θ_2 adjustment is 2 minutes of arc, which is experimentally feasible with a standard high-resolution rotation stage. The angular excursion is converted into relative phase delay by taking into account beam refraction inside the calcite, and we find the period to be 2.6 fs, which corresponds to the period of the laser electric field.

The influence of gas pressure inside the fiber was investigated as shown on Fig. 3. When Ne gas is added with a pressure ranging from 0 to 2.5 bar, the spectrum progressively broadens as expected [Fig. 3(a)]. The 70% fiber transmission remains constant as no ionization occurs. Systematic recording of the fringed spectra [Fig. 3(b)] shows that the increased nonlinear broadening of the pulse replicas inside the fiber does not affect their relative phase. The combining efficiency stays above 90% for all pressures. The sudden recovery of efficiency at 1.75 bar is due to realignment of the setup with increasing gas pressure. At the optimum Ne pressure of 2 bar, we obtain a spectrum with 166-nm FWHM and a combining efficiency of 95%. The energy of the combined pulse is then 0.62 mJ but could be even higher using a better AR-coating on the second calcite plate. We identify three main contributions to the overall losses: the inherent fiber transmission losses, the AR-coating of both plates, and the combination losses embedded in the overall transmission of the TFP.

Looking at the θ-scan curve for 2 bar of Neon [Fig. 2(a)], we notice that the oscillation envelope is shorter than in the case of vacuum. This is due to the

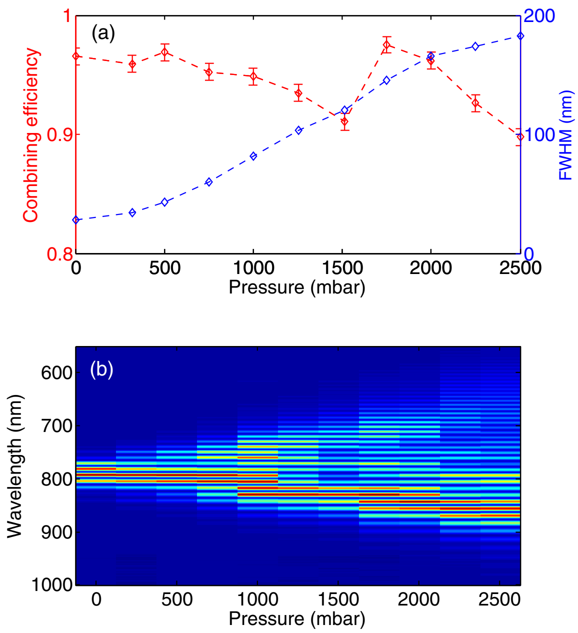

Fig. 3. (a) Evolution of the combining efficiency and spectral bandwidth of the combined pulse as a function of Ne pressure. (b) Evolution of the fringed spectrum as a function of Ne pressure.

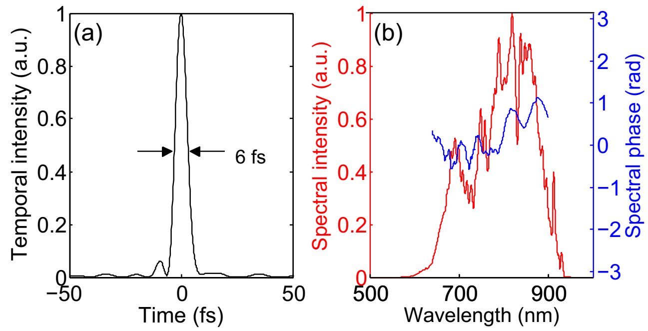

Fig. 4. Characterization of the combined pulse: (a) temporal intensity and (b) spectral intensity and phase.

much broader spectrum of the combined fields. The oscillation period of the combining efficiency varies as the central wavelength of the pulse shifts due to the nonlinear spectral broadening process. Fig. 2(b) shows the fringed spectrum together with the combined spectrum [Fig. 2(b)]. The fringed spectrum is deeply contrasted over the whole bandwidth demonstrating that the two replicas undergo similar nonlinear broadening in the fiber. Combining in the calcite plate enables the phase-matching of the newly created wavelengths with remarkable stability as shown on Fig. 2(b), where 500 consecutive combined spectra recorded with 10-ms integration time are superimposed. The long-term energy stability of the combined pulse is 1.8% RMS over more than 3 h, which is directly related to the pump laser fluctuations inside the Femtopower.

The compressed recombined pulse was temporally characterized with a Wizzler-USP (Fastlite) measurement [14], as shown in Fig. 4. A 6-fs pulse was obtained for a Ne pressure of 2 bar. The spectral phase is globally flat with residual oscillations introduced by the chirped mirrors. The high dynamic range of the Wizzler-USP device allows the optimization of the temporal pulse shape by adjusting α_2. At the optimal α_2 value (0°), no pre-pulse at −178 fs is measured above 10^{-3} relative intensity [Fig. 5(a)], demonstrating the efficiency of the combining process. Away from this optimal value, the pre-pulse intensity increases. At 10^{-2} relative intensity, a weak residual modulation starts to become visible on the combined fringed spectrum [Fig. 5(b)].

Finally, it is necessary to confirm that the CEP stability of the combined pulse is preserved. The CEP was measured with a home-made f-to-2f interferometer interfaced with a spectrometer and analysis software from Menlo Systems. The CEP noise of the 6-fs pulse is about 180-mrad RMS for an integration time of 1 ms and a slow feedback period of 48 ms [Fig. 6(a)], which is comparable to that of the input pulses from the amplifier. Moreover, we measured the CEP of a single pulse propagating through the fiber and exhibiting the same broadened spectrum [Fig. 6(b)]. Given the intrinsic noise of the f-to-2f device, the CEP drifts are of the same order of magnitude in both configurations confirming that no measurable CEP noise is introduced by the recombination process.

In summary, we demonstrated passive combining of few-cycle pulses in a hollow fiber compressor. A first calcite plate is used to temporally divide the input pulse

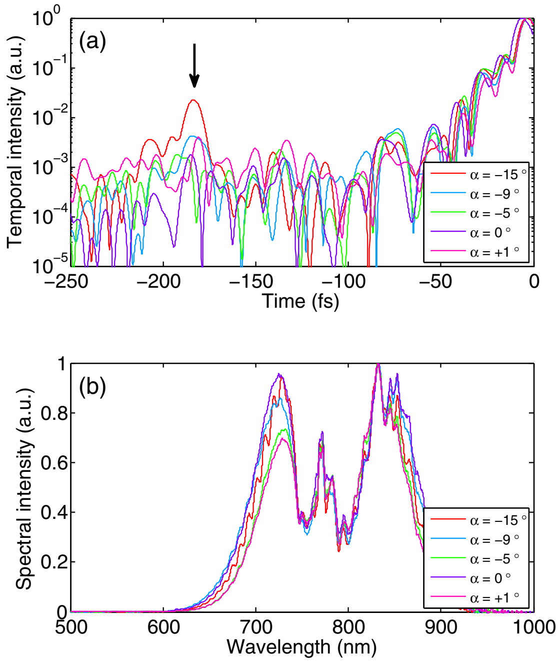

Fig. 5. Wizzler measurement of the combined pulse for various α_2 values: (a) temporal intensity profile (logarithmic scale), (b) corresponding spectra.

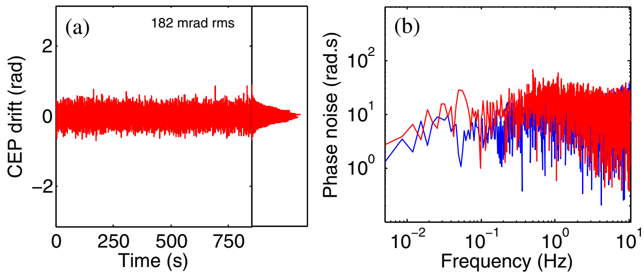

Fig. 6. (a) Relative CEP drift of the combined pulse after temporal post-compression with slow feedback on the stretcher. (b) Fourier analysis of the CEP noise registered for post-compressed single pulse (blue, 145-mrad RMS) and two combined replicas (red, 182-mrad RMS).

into two temporal replicas with lower energy. At optimal gas pressure, a combining efficiency of 95% can be achieved by simply tuning the orientation of a second calcite plate used for recombination. CEP noise is about 180-mrad RMS, and the combined pulse duration is 6 fs with excellent passive stability. Our setup fulfills two basic requirements for efficient coherent combining of few-cycle pulses: temporal fidelity over several orders of magnitude and CEP stability. Combining of two pulses should allow a twofold increase in the throughput energy of already existing hollow fiber compressor systems with stable CEP. We are currently investigating the experimental limits of higher pulse multiplexing as a viable energy scaling tool for hollow fiber compressors.

The authors thank Fastlite for the loan of the Wizzler-USP device. Financial support from Conseil Régional d'Ile-de-France and ELI-HU Nonprofit Ltd. is gratefully acknowledged.

References

1. F. Krausz and M. Ivanov, Rev. Mod. Phys. **81**, 163 (2009).
2. M. Nisoli, S. De Silvestri, and O. Svelto, Appl. Phys. Lett. **68**, 2793 (1996).
3. S. Sartania, Z. Cheng, M. Lenzner, G. Tempea, C. Spielmann, F. Krausz, and K. Ferencz, Opt. Lett. **22**, 1562 (1997).
4. F. Böhle, M. Kretschmar, A. Jullien, M. Kovacs, M. Miranda, R. Romero, H. Crespo, U. Morgner, P. Simon, R. Lopez-Martens, and T. Nagy, Las. Phys. Lett. **11**, 095401 (2014).
5. D. Wang, Y. Leng, and Z. Huang, J. Opt. Soc. Am. B **31**, 1248 (2014).
6. S. Szatmari and P. Simon, Opt. Commun. **98**, 181 (1993).
7. L. Daniault, M. Hanna, L. Lombard, Y. Zaouter, E. Mottay, D. Goular, P. Bourdon, F. Druon, and P. Georges, Opt. Lett. **36**, 621 (2011).
8. Y. Zaouter, L. Daniault, M. Hanna, D. Papadopoulos, F. Morin, C. Hönninger, F. Druon, E. Mottay, and P. Georges, Opt. Lett. **37**, 1460 (2012).
9. S. Bagayev, V. Leshchenko, V. Trunov, E. Pestryakov, and S. Frolov, Opt. Lett. **39**, 1517 (2014).
10. A. Klenke, M. Kienel, T. Eidam, S. Hädrich, J. Limpert, and A. Tünnermann, Opt. Lett. **38**, 4593 (2013).
11. F. Guichard, Y. Zaouter, M. Hanna, F. Morin, C. Hönninger, E. Mottay, F. Druon, and P. Georges, Opt. Lett. **38**, 4437 (2013).
12. S. W. Huang, G. Cirmi, J. Moses, K.-H. Hong, S. Bhardwaj, J. R. Birge, L.-J. Chen, E. Li, B. J. Eggleton, G. Cerullo, and F. Kärtner, Nat. Photonics **5**, 475 (2011).
13. V. E. Leshchenko, V. I. Trunov, S. A. Frolov, E. V. Pestryakov, V. A. Vasiliev, N. L. Kvashnin, and S. N. Bagayev, Las. Phys. Lett. **11**, 095301 (2014).
14. A. Moulet, S. Grabielle, C. Cornaggia, N. Forget, and T. Oksenhendler, Opt. Lett. **35**, 3856 (2010).